Title: Of mice and motion: Behavioural-EEG phenotyping of Alzheimer's disease mouse models

Authors: Barry Crouch, Jie Min Yeap, Bianca Pais, Gernot Riedel, Bettina Platt

PII: S0165-0270(18)30206-1
DOI: https://doi.org/10.1016/j.jneumeth.2018.06.028
Reference: NSM 8050

To appear in: *Journal of Neuroscience Methods*

Received date: 27-4-2018
Revised date: 14-6-2018
Accepted date: 28-6-2018

Please cite this article as: Crouch B, Yeap JM, Pais B, Riedel G, Platt B, Of mice and motion: Behavioural-EEG phenotyping of Alzheimer's disease mouse models, *Journal of Neuroscience Methods* (2018), https://doi.org/10.1016/j.jneumeth.2018.06.028

Special Issue:
Methods and Models in Alzheimer's Disease Research

Of mice and motion: Behavioural-EEG phenotyping of Alzheimer's disease mouse models

Barry Crouch, Jie Min Yeap, Bianca Pais, Gernot Riedel & Bettina Platt*

Institute of Medical Sciences,

School of Medicine, Medical Sciences & Nutrition

University of Aberdeen, Foresterhill, Aberdeen AB25 2ZD, United Kingdom

* Corresponding author
Contact:
Tel: .(+44) 1224 437402
Email: b.platt@abdn.ac.uk

Highlights

- Event stamping enables alignment between behavioural observation and EEG sampling.
- Speed and motion modulate autoregressive EEG spectra.
- Controlling for speed is critical when quantifying EEG.
- Hippocampal EEG Gamma response to speed is deficient in Alzheimer mice.
- EEG response to direction remain intact in Alzheimer mice.
- EEG response to correct vs incorrect y-maze alternations is affected in transgenic mice.

Abstract

Background: Rodent electroencephalography (EEG) in preclinical research is frequently conducted in behaving animals. EEG analysis is complicated by a number of confounds, particularly 1. The close relationship between EEG power and movement speed must be controlled for prior to further analysis. 2. The difficulty inherent in identifying EEG epochs associated with a particular behaviour.

New Method: We utilized infra-red event stamping to accurately synchronize EEG recorded from superficial sites above the hippocampus and prefrontal cortex with motion tracking data in a transgenic Alzheimer's disease (AD) mouse model ($PLB1_{APP}$) and wild-type controls (PLB_{WT}) performing

a Y-maze spontaneous alternation task. Video tracking synchronized epochs capturing specific behaviours were automatically identified and extracted prior to auto-regressive spectral analysis.

Results: Despite comparable behavioural performance, $PLB1_{APP}$ mice demonstrated region and behavioural context specific deficits in regulation of Gamma power: In contrast to controls, hippocampal gamma response to speed as well as prefrontal activity associated with correct vs. incorrect alternations was absent in $PLB1_{APP}$ mice. Regulation of hippocampal Gamma power in response to direction of movement did not differ.

Comparison with existing Methods: This method allows for the first time to detect behaviour-specific differences in EEG response to speed that can be quantified and actively controlled for. Analysis across multiple parameters engaging different brain regions can now be used for detailed EEG profiling of brain-region specific functions.

Conclusion: Combining infrared event-stamping and auto-regressive modelling enables rapid, automated and sensitive phenotyping of AD mouse models. Subtle alterations in brain signalling can be detected prior to overt behavioural impairments.

Keywords:

EEG, behaviour, spectral analysis, autoregressive modelling, theta, gamma, speed, motion, Y-maze, amyloid precursor protein

1. Introduction

Functional magnetic resonance imaging (fMRI) and quantitative electroencephalography (qEEG) are common, non-invasive techniques for quantitative analysis of brain activity. Both techniques confer individual advantages in human research dependent upon whether temporal (qEEG) or spatial (fMRI) resolution of brain signals is the more critical consideration. However, as EEG apparatus are inexpensive and highly portable relative to MRI scanners, they confer a distinct advantage in clinical practice. EEG recording is non-invasive and can be performed in the laboratory, the clinic, the home and at the bedside. qEEG therefore offers the potential for cost-effective, compassionate diagnosis and monitoring of Alzheimer's disease (AD). Additionally as EEG recording is easily applicable to rodent disease models and can be conducted in awake animals. qEEG is therefore considered a promising approach to discovery of translational biomarkers (Drinkenburg et al., 2016; Leiser et al., 2011; Platt et al., 2011b).

Numerous studies have observed characteristic EEG changes in dementia patients including; Slowing of the EEG (increased delta-theta and decreased alpha-gamma power), reduced EEG complexity, and reduced functional connectivity between brain regions (Hamm et al., 2015; Jeong, 2004). Regarding EEG slowing, it is thought that increased theta and reduced beta power emerge in early AD while increased delta occurs at more advanced stages of the disease (Coben et al., 1985). Few human studies have expressly investigated changes in gamma activity, although this is largely due to poor agreement between studies regarding frequency band definitions where slow gamma frequencies (20-35 Hz) are often considered a high frequency beta subtype. Nevertheless, increases in the ratio of Theta to Gamma power are correlated with memory decline in mild cognitive impairment (MCI) and may provide an early predictor of progression from MCI to AD (Moretti et al., 2009). Furthermore, as EEG changes in AD track cognitive function, EEG may offer a valuable diagnostic of disease progression

with significant applications in quantifying efficacy of novel therapeutics at both the clinical and preclinical level.

1.1 - Hippocampal / Entorhinal Gamma power in AD

There is strong evidence from both human AD and animal models that the entorhinal cortex (EC) is heavily damaged in AD with pathological changes occurring very early in the disease course (Braak and Braak, 1991; Khan et al., 2014). An EEG based diagnostic of EC function could therefore be immensely valuable in preclinical research and ultimately, in early diagnosis. Aside from functions related to memory, the EC has been an area of intense study in rodents due to the key role played by the EC in encoding the location of the animal within an environment as well as speed and trajectory of movement to enable navigation (Hinman et al., 2018; Moser et al., 2008). Studies of local field potentials in transgenic mouse models of AD have revealed both reduced Gamma power and frequency in the lateral EC (Klein et al., 2016). Dysfunction of Theta-Gamma cross frequency coupling in medial EC layers 2 and 3 (Nakazono et al., 2017) and dysfunction of medial EC grid cells (Fu et al., 2017). Probing the regulation of hippocampal EEG in response to movement (encoded primarily by the EC) may therefore provide an easily accessible diagnostic of hippocampal / entorhinal function in translational mouse models of AD.

Recording of local field potentials are comparatively rare in mice where superficial recording electrodes are more commonly deployed for sleep, circadian activity and pharmaco-EEG research. Hippocampal EEG activity is therefore usually represented by a skull embedded electrode anchored above the CA1. The CA1 gamma rhythm, generated by cells proximal to the superficial recording electrode, is thought to be entrained by inputs from the CA3 and EC (Colgin, 2016). It may therefore be possible to distinguish EC from either CA3 or CA1 dysfunction through examination of CA1 Gamma power modulation in response to behavioural demands which differentially engage the CA3 and EC. Additionally, it has long been established that the hippocampus proper, EC and dentate follow a common theta rhythm regulated by input from the medial septum which acts as a common pacemaker (Buzsáki, 2002; Colgin, 2016; Freund and Antal, 1988). The observation that both hippocampal theta and CA1 gamma are highly correlated with movement speed (Chen et al., 2011; McFarland et al., 1975) further indicates that the regulation of both hippocampal theta and Gamma power with locomotive factors could be adequately quantified using a superficial recording electrode. Additionally while the human hippocampus and EC are difficult to access with superficial recording electrodes, intracranial recording of the hippocampus in human participants has demonstrated that the human hippocampal theta rhythm is also modulated by (simulated) movement (Bush et al., 2017; Watrous et al., 2011). These findings provide evidence that observations of hippocampal oscillatory changes with movement in rodents may be directly translatable to humans.

1.2 Challenges in pre-clinical behavioural EEG

Recent advances in miniaturization of wireless EEG recording devices (Crispin-Bailey et al., 2013; Etholm et al., 2010) enable brain activity to be recorded in freely moving animals in a range of environments. However, the combination of behavioural / cognitive testing and qEEG in rodents is arguably more complex than in human subjects. A human participant can be instructed to comply with the rules of a task, technical requirements (lie still with eyes closed etc.) and to provide responses at designated time points. Reproducible EEG epochs which fit designated criteria can therefore be identified and extracted with relative ease. By contrast, in pre-clinical rodent research, one has little to no control over when or if an animal may express a particular behaviour. This is doubly true of

experiments in 'freely behaving' animals such as home cage recordings, open fields or spontaneous alternation tasks. One must hope therefore that;

1. An animal will perform the desired behaviours a sufficient number of times for analysis.
2. That EEG corresponding to these behaviours can be accurately located in time.
3. That behaviour during these events is largely homogeneous between samples.

The challenge imposed by point 1 is magnified by traditional approaches to qEEG analysis. Spectral analysis is usually based upon Fourier transformation of the signal to calculate EEG amplitude (power) in the frequency domain usually using the fast Fourier transform (FFT). The FFT is particularly vulnerable to noise within the signal and windowing artefacts. Averaging over a large number of epochs is therefore required to achieve a reliable power spectral estimate inflating the volume of data required for analysis. Use of the FFT also carries some less obvious implications related to point 2. The FFT is subject to time-frequency Heisenberg uncertainty whereby epochs which can more accurately isolate a behavioural event in time consequently reduce frequency resolution. Similarly, the spatial location and velocity of an animal must be averaged over the length of the EEG epoch. One must therefore attempt to strike an acceptable balance between certainty of an animal's behaviour and the frequency resolution of the corresponding EEG analysis.

1.3 Rapid behavioural EEG phenotyping of transgenic mouse lines

In a recent publication (Crouch et al., 2018) we demonstrated the use of Autoregressive (AR) spectral estimation in pre-clinical EEG applications. AR methods offer an alternative to the FFT which carry the added advantage of resistance to noise and spectral leakage (Faust et al., 2008). Additionally, the frequency resolution of AR analysis is not directly related to window length. As a consequence, cleaner spectra can be produced using fewer, shorter epochs. We also demonstrated the use of Infra-red event-stamping to enable synchronization of EEG data with behavioural tracking software. This process enables one to automatically identify epochs during which behaviour fits rigorous selection criteria. Behavioural homogeneity between samples is therefore maximized and major confounding influences such as differences in locomotor activity between samples can be minimized. This latter consideration has particular relevance in analysis of hippocampal Gamma / Theta activity which are highly sensitive to movement speed.

In this manuscript, we shall demonstrate that the combination of these techniques can enable simultaneous, high-throughput profiling of EEG response to a range of behavioural parameters in transgenic mouse models. Specifically, we shall investigate the relationship between EEG power and; **locomotive** (movement speed), **navigational** (direction of movement) and **cognitive** (spatial decision making) factors in the $PLB2_{APP}$ mouse models of AD during a Y-maze continuous spontaneous alternation task (Hughes, 2004).

2. Methods

2.1 Animals and surgical procedures

$PLB2_{APP}$ mice are human mutated amyloid precursor protein (APP) expressing models of Alzheimer's disease (AD) bearing a single copy of the human APP with both the Swedish and London mutations (CaMKIIα promoter). They were derived from deleter breeding of a previously described double (APP+Tau) mutant line (Platt et al., 2011a). At this age point, $PLB2_{APP}$ mice exhibit mildly increased

intra and extracellular deposition of β-amyloid in the forebrain as well as pronounced astrogliosis in the CA1 and dentate gyrus. Of note, these histological features observed in ~6-month old $PLB2_{APP}$ mice occur without formation of aggregated amyloid plaques or frank neuronal loss (Plucińska et al., *in press*). $PLB2_{APP}$ mice at this age are therefore taken as a model of early AD pathology.

All procedures were conducted as outlined previously (Crouch et al., 2018). Briefly, 9 female $PLB2_{APP}$ mice underwent electrode implantation surgery at 5 months of age, alongside 9 age and gender matched wild-type controls ($PLB1_{WT}$). Four gold screw electrodes were bilaterally implanted under general anaesthesia (isoflurane) into the skull at stereotaxic co-ordinates (Paxinos and Franklin, 2004) above the prefrontal cortex (2 mm anterior to Bregma immediately left and right of midline) and hippocampus (2 mm posterior, ±1.5 mm lateral to Bregma). Two reference electrodes were also placed at neutral posterior locations in the parietal plates. Data presented in this study are from the left hemisphere recording sites. Subcutaneous buperinorphine was administered for prophylactic pain relief prior to recovery from general anaesthesia. For 48 hours after surgery, the animals' drinking water was also supplemented with carprofen to provide minimally invasive anti-inflammatory support. Behavioural testing was conducted 2 weeks after implantation. Animals were housed and tested in accordance with European (FELASA) and UK Home Office regulations. All experiments were approved by the University's Ethics Board and carried out in accordance with the Animal (Scientifc Procedures) Act 1986 and EU directive 2010/63/EU.

2.2 Behavioural testing + EEG recording

EEG activity was recorded at a sampling rate of 200 Hz using the NAT-1 wireless recording device (Cybula, UK; (Crispin-Bailey et al., 2013)) during a Y-maze spontaneous alternation task. NAT-1 devices were attached under gentle manual restraint and animals were allowed 30 minutes habituation to the device and experimental room prior to testing. The Y-maze itself consisted of 3 open-topped corridors (A, B and C) each 60cm in length, meeting at a triangular intersection (Plucińska et al., 2014). Testing consisted of a single 10 minute trial where each sequence of 3 consecutive arm entries made by the animal was recorded by an observer as either a 'correct alternation' (ABC etc), an 'incorrect alternation' (ABA etc) or a 'direct repetition' (AAB) as per (Crouch et al., 2018; Thompson et al., 2005). The number of correct alternations as a percentage of all alternations was taken as an index of cognitive performance. Total distance moved and average speed were also recorded for analysis of locomotor function. Motion tracking was conducted using an overhead camera connected to a computer running the Anymaze 5.0 (Ugo Basile, Italy) software package.

2.3 Behavioural + EEG data synchronization

Precise synchronization of motion tracking and EEG data was performed as outlined in (Crouch et al., 2018). Briefly, 7 virtual zones representing the inner and outer half of each arm and their area of intersection were defined in ANYMAZE. Transition of the animal across a zone boundary triggered a TTL output via an ANYMAZE interface (AMI) module (Ugo Basile, Italy). These TTL pulses then activated pulses of infra-red (IR) light from an overhead IR LED array which were received by the NAT-1s on-board IR receiver. After completion of the experiment, a test data report containing a complete record of the animal's spatial co-ordinates and TTL activations alongside the real time indices (RTIs) of these data were then exported from ANYMAZE in .csv format. An in-house MATLAB (Mathworks, USA) script was then used to match the real time RTI of each TTL activation to the corresponding activation of the NAT-1's IR channel. EEG samples corresponding to the onset of IR signals could then be tagged with RTIs. Time indices of EEG samples between IR activations were then interpolated. The animal's co-ordinates and behaviour could then be calculated for each EEG sample through cross-referencing the RTI of the sample with the record of the animal's behaviour at the closest RTI logged in the test data

report. As behavioural data were updated by ANYMAZE at 12 times each second, this defines the temporal resolution of the animal's location.

2.4 Data processing

EEG band definitions were: Delta 0.5-5Hz, Theta 5-9 Hz, Alpha 9-14 Hz, Beta 14-20 Hz and Gamma 20-40 Hz. Once synchronized to tracking data, each subject's EEG recordings was divided into a set of discrete 4 second epochs. This epoch length was selected as a 4s window was short enough to be appropriately applicable for all behavioural parameters investigated here, while long enough to sufficiently minimize the potential impact of any lag in registration of movement by the tracking software. An autoregressive (AR) power spectrum with frequency resolution = 0.5 Hz was then calculated for each epoch using an AR order of 50 samples (sampling rate / 4) as previously described (Crouch et al., 2018). The animals' speed and direction of motion relative to the maze centre point during each epoch were also calculated. Power spectra were first averaged within subjects over all available epochs and the result normalized to total power to create a *general power spectrum* for each subject. Comparison of general power spectra between genotypes was used to screen for any overall effect of genotype on EEG power regardless of behavioural context.

2.5 Effect of movement speed on EEG power

Each subject's set of 4s EEG epochs were first ordered by speed. As there was some heterogeneity between subjects in terms of maximum speed, setting an upper speed limit was necessary to enable a fair comparison across subjects. Additionally, inordinately high speeds detected within an epoch may be attributable to tracking artefacts. Therefore, epochs with speed > 16 cm/s were rejected. This threshold was set on the basis that epochs with speed > 16 cm/s were detected for each animal ensuring that analysis would only be conducted over a range of speeds achievable by all subjects. Remaining epochs were then sorted into 5 linearly spaced speed bins: **S1** = 0-3.2 cm/s, **S2** = 3.2-6.4 cm/s, **S3** = 6.4-9.6 cm/s, **S4** = 9.6-12.8 cm/s and **S5** = 12.8-16 cm/s and the average AR power spectrum was calculated for each speed bin. Element-wise division of each subjects S5 spectrum by its S1 spectrum creates a *relative power spectrum,* where values above 1 of the resultant spectrum indicate power is higher at high speed while those below 1 indicate power is higher at low speed. For statistical analysis of genotype differences in EEG response to speed, EEG bands were first condensed to mean band powers to represent each band as a single point. Comparison of *relative band power* (S5 band powers / S1 band powers) between genotypes was then conducted via 2-way ANOVA for each recording site.

Analysis of S1 and S5 alone represents a comparison of EEG power difference between opposite ends of an animal's speed range. In order to establish whether this difference is proportionately related to speed, rather than simply due to (for example) some factor occurring specifically during high speed movement, it is necessary to observe EEG power over a range of speeds. To accomplish this, band power at all speed bins was normalized within subjects relative to S1. The Pearson's correlation coefficient over S1-S5 was then determined to probe the relationship between EEG band power and speed.

2.6 Effect of direction and alternation type on EEG power

To examine the EEG response to direction of motion, we compared EEG band power during motion towards vs motion away from the maze centre. To nullify any confounding influence of speed, epochs representing inward and outward motion in the analysis had to be well balanced for speed. Here, we utilized a simple heuristic approach based on spatial displacement to select appropriate epochs. 4s epochs where the final position of the animal was >=50cm closer to the centre of the maze than at

the start of the epoch (inward displacement), were used to represent inward motion. Similarly, epochs with >=50cm of outward displacement were used to represent outward motion. Motion plots presented in Fig. 1 demonstrate that, due to the construction of the Y-maze, this simple rule ensures that selected epochs are composed of constant, unidirectional motion. Any confounding influence of speed was therefore nullified. Comparison of relative band power (inward / outward) between genotypes as then conducted via 2-way ANOVA was used to compare EEG response to direction. One-sample 2-tailed t-tests of relative band powers against a chance level of 1 were also used to test for a significant effect of direction within each genotype.

Finally, 6 of the previously described outward motion epochs were selected from each subject, 3 which represented the completion of a correct alternations and 3 of an incorrect alternation. Speed and direction during correct and incorrect samples were therefore controlled by default. Analysis of relative band power (Incorrect / correct) was conducted and analysed exactly as in the previous inward vs outward analysis.

3. Results

3.1 Behavioural parameters

The number of correct alternations, as % all alternations (Fig. 2 A) did not significantly differ between $PLB1_{WT}$ and $PLB2_{APP}$ mice [F<1] nor was any significant genotype-alternation type interaction observed [F(2,48) = 1.695, p>0.05]. Crucially, the effect of alternation type was highly significant [F(2,48) = 256.0, p<0.001] with correct alternations more common than incorrect in both genotypes [$PLB1_{WT}$: t(8) = 2.555, p<0.05, $PLB2_{APP}$: t(8) = 2.457 p<0.05]. Comparison of total distance travelled over the duration of the y-maze experiment (Fig. 2 B) revealed no significant genotype differences [t<1]. Average speed (Fig. 2 C), being simply distance moved over 10 mins, was therefore also equivalent between genotypes.

3.2 General EEG power spectra during Y-maze task

Despite the apparent lack of a cognitive phenotype, analysis of absolute (raw) EEG power (Fig. 3 A+C) recorded by both prefrontal and hippocampal electrodes indicated that $PLB2_{APP}$ mice exhibit globally lower absolute power than $PLB1_{WT}$ controls across the entire spectrum (prefrontal [F(1,1280) = 386.4, p<0.001], hippocampus [F(1,1280) = 368.9, p<0.001]). Normalization to total power (Fig. 3 B+D) indicated that the power spectra of $PLB2_{APP}$ mice indeed contain proportionately less Beta + Gamma and more Delta + Theta power cf. $PLB1_{WT}$ mice. This slowing of the EEG (redistribution of energy from higher to lower frequency bands) is in accordance with EEG biomarkers of dementia observed in the human condition.

3.3 Modulation of EEG power with movement speed

Plots in Fig. 4 A+D display relative power spectra obtained through element-wise division of each animals highest speed (S5) power spectrum by its lowest speed (S1) spectrum. Values above 1 (horizontal dashed line in Fig. 4 A+D) therefore indicate that EEG power at the associated frequency is higher during S5 (highest speed) than S1 (lowest speed) epochs. Conversely, values below 1 indicate higher power during S1 than S5 epochs. Visual examination of these plots demonstrate that for **$PLB1_{WT}$ mice**, at both recording sites, Delta, Alpha and low Theta range power were reduced at high speed while high Theta range power was increased. Gamma power was also increased at high speed in the hippocampal recording site, as was Beta power albeit specifically in a narrow peak centred at 16.5 Hz. Similar effects of speed on Delta, Theta and Alpha power were also observed in $PLB2_{APP}$ mice.

However, (in contrast to $PLB1_{WT}$), **$PLB2_{APP}$** hippocampal Beta and Gamma power was broadly equivalent between S1 and S5 epochs. Subsequent statistical comparison of the corresponding relative band power data (Fig. 4 B+E) confirm that the effect of speed on EEG power significantly differs by band [prefrontal : $F(4,80) = 3.429$, $p<0.05$, hippocampus : $F(4,80) = 17.910$, $p<0.001$]. No significant effect of genotype was detected in the prefrontal recording site [$F<1$], but a significant effect of genotype was detected for the hippocampal channel [$F(1,80)=4.477$, $p<0.05$], alongside a significant band-genotype interaction [$F(4,80) = 4.377$, $p<0.01$]. Bonferroni post-tests confirmed that $PLB2_{APP}$ significantly differed from $PLB1_{WT}$ in hippocampal gamma response to speed [$t=3.440$, $p<0.01$].
To further clarify the relationship between gamma power and speed, mean gamma band power observed at each velocity bin was normalized within subjects to velocity bin 1 (Fig. 4 C+F). Correlation analysis revealed, that in $PLB1_{WT}$ mice, hippocampal Gamma power was significantly positively correlated with movement speed while prefrontal Gamma power was not [Hippocampus : $r = 0.9514$, $p<0.05$, Prefrontal cortex : $r = -0.4450$, $p>0.05$]. By contrast, $PLB2_{APP}$ displayed no correlation between speed and Gamma power in either the prefrontal cortex [$r = -0.8023$, $p>0.05$] or hippocampus [$r = -0.8230$, $p>0.05$].

As the effect of speed on hippocampal Theta and Beta power varies greatly with frequency within these bands (Fig. 4 D), analysis of mean band power alone is misleading. To better quantify speed related phenomena within these bands we therefore investigated next the correlations between speed and peak (highest power detected at any frequency point within a band) power (Fig. 5). Interestingly, while hippocampal peak Theta power directly correlated with movement speed in both $PLB1_{WT}$ [$r= 0.09878$, $p <0.01$] and $PLB2_{APP}$ mice [$r = 0.9435$, $p<0.05$], peak Beta power was also directly related to speed in $PLB1_{WT}$ mice (marginally failing significance, $r = 0.8698$, $p = 0.0553$] and no such trend was observed in $PLB2_{APP}$ mice [$r = -0.3832$, $p>0.05$].

Cumulatively, these results indicate that the modulation of hippocampal Delta - Alpha power with movement speed is intact in $PLB2_{APP}$ mice, while Gamma (and Beta) power modulation is impaired.

3.4 Modulation of Gamma power with direction of motion (inward vs outward)

The analysis of EEG mean band power during inward motion measured relative to outward motion is presented in Fig. 6 A+C. Scatter plots elaborating upon the effect of direction specifically on gamma power are presented in Fig. 6 B+D. Two-tailed one-sample t-tests against a chance level of 1 revealed that both genotypes demonstrated significantly higher prefrontal Gamma power during inward motion than during outward [$PLB1_{WT}$: $t(8) = 2.783$, $p<0.05$, $PLB2_{APP}$: $t(8) = 4.138$ $p<0.01$]. The same was also true of Hippocampal gamma power [$PLB1_{WT}$: $t(8) = 2.783$, $p<0.05$, $PLB2_{APP}$: $t(8) = 3.380$ $p<0.01$]. Comparison of Gamma power modulation between genotypes also revealed no significant difference in either recording site [both $t<1$]. Neither was any effect of genotype or interaction identified at lower frequency bands [all F's <1]. Therefore, while regulation of hippocampal Gamma with speed is deficient in $PLB2_{APP}$ mice, when the influence of speed is appropriately controlled for, the hippocampal gamma responses to direction of motion appears intact.

3.5 Modulation of EEG power with alternation type (correct vs incorrect)

Inspection of prefrontal mean band power during the third arm entry of incorrect vs incorrect alternation triplets (relative band power, Fig 7 A+D) illustrate that the two genotypes did not differ [$F(1,80) = 1.255$, $p>0.05$], and no significant genotype-band interaction was detected [$F<1$]. Similarly, analysis of hippocampal relative band power revealed no significant overall effect of genotype [$F<1$]. However, in this case a significant interaction was observed [$F(4,80) = 4.829$, $p<0.01$], which was attributable to a difference in the Alpha band [Bonferroni post-test: $t = 3.331$; $p<0.01$]. In accordance with our previous observations, prefrontal Gamma power (Fig. 7 C) was higher for incorrect than

correct alternations in $PLB1_{WT}$ mice [t(8) = 3.242, p<0.05], while the same was not true of $PLB2_{APP}$ mice [t(8) = 1.260, p>0.05]. However, the genotypes did not significantly differ when compared directly [t(16) = 1.342, p>0.05]. No significant effect of alternation type on hippocampal gamma power (Fig. 7 F) was detected for either genotype [$PLB1_{WT}$: t<1, $PLB2_{APP}$: t(8) = 1.492, p>0.05].

One sample t-tests conducted against chance further confirmed that $PLB1_{WT}$ mice displayed higher Alpha power in incorrect relative to correct alternations in both the hippocampus [t(8) = 3.039, p<0.05] and prefrontal cortex [t(8) = 2.354, p<0.05] while the same was not true of $PLB2_{APP}$ mice [both t<1] (see Fig. 7 B+E). Direct comparison confirmed that $PLB1_{WT}$ and $PLB2_{APP}$ mice differed in relative hippocampal Alpha power [t(16) = 3.048, p<0.01] but not prefrontal relative alpha power [t(16) = 1.054, p>0.05]. Similar results were also obtained for hippocampal Beta activity with $PLB1_{WT}$ but not $PLB2_{APP}$ mice demonstrating higher power in incorrect than correct alternations [$PLB1_{WT}$: t(8) = 2.341, p<0.05, $PLB2_{APP}$: t<1]. Relative hippocampal beta power was also significantly different between genotypes under direct comparison [t(16)=2.456, p<0.05]. Therefore, while genotypes are equivalent in terms of alternation score, $PLB1_{WT}$ mice express clear patterns of brain activity differentiating correct from incorrect alternations, $PLB2_{APP}$ mice do not.

4. Discussion

We here demonstrate that a combination of synchronizing EEG with video tracking enables rapid behavioural qEEG profiling of experimental cohorts based on autoregressive modelling, to detect alterations in brain signalling in the absence of overt behavioural changes. Using this approach, one can quantify EEG power modulation with a behavioural parameter (e.g. speed, heading, etc) within individual subjects. We have also demonstrated that controlling for the influence of speed during epoch selection is critical to enable a meaningful comparison of EEG phenotypes between test groups. Furthermore, we show that genotype differences in response to one parameter (e.g. speed) does not confound further analysis if controlled for through automated, 'intelligent' (rule based) selection of epochs to nullify the influence of confounding parameters.

The key findings of our study, discussed consecutively below, are that under speed controlled phenotypic comparison: **1.** Hippocampal Gamma power is directly correlated with movement speed in $PLB1_{WT}$ but not $PLB2_{APP}$ mice. **2.** Both genotypes demonstrate enhanced prefrontal and hippocampal Gamma while moving towards the centre of the Y-maze arena. **3.** Incorrect spontaneous alternations are associated with elevated prefrontal Gamma and globally elevated Alpha power in $PLB1_{WT}$ but not $PLB2_{APP}$ mice. **4.** Genotype differences emerged amidst equivalent task performance.

While the pathological origins of any phenotypic changes require further histological and molecular confirmation (see Plucińska et al., *in press*, for further information), we shall here discuss how our findings can guide further functional studies through identifying brain regions of interest.

4.1 Hippocampal gamma power and speed

The CA1 Gamma rhythm is thought to be composed of at least 2 distinct oscillatory bands termed slow (~25-55 Hz) and fast (~60-100 Hz) Gamma (Colgin, 2016). The Gamma band analysed here corresponds to both the frequency definitions and linear speed-amplitude response characteristics reported of CA1 slow gamma in mice (Chen et al., 2011). CA1 slow Gamma is therefore the likely source of speed modulated Gamma activity reported here in $PLB1_{WT}$ mice. Multiple lines of evidence suggest that CA1 slow Gamma is entrained by corresponding oscillations in the CA3 while CA1 fast Gamma is entrained by the EC (Colgin, 2016; Colgin et al., 2009; Schomburg et al., 2014). Furthermore, activation of CA1

place cells by the EC's fast Gamma is thought to encode information regarding the animal's current position and trajectory while activation by CA3's slow Gamma encodes representations of upcoming trajectories (Zheng et al., 2016).

Current speed is encoded by grid and speed cells in the medial EC (Hinman et al., 2018; Kropff et al., 2015), hence the CA1's representation of speed should be encoded in fast Gamma. However, both our own findings and those of Chen et al (2011) demonstrate that locomotion drives CA1 slow Gamma This may be due to species differences in rats vs mice regarding projections from the EC to the CA3 (Ahmed and Mehta, 2012, 2009). Given that CA1 receives the same EC input both directly and indirectly via the CA3, the distinction between the roles of fast and slow CA1 Gamma may not be as rigid in mice. Consequently, the impaired regulation of CA1 gamma with speed in $PLB2_{APP}$ mice could be attributable to dysfunction of the EC (in line with previous evidence from other AD mouse models), the CA3 or the CA1. Investigation of EEG response to other parameters however may shed further light on the matter. Interestingly, $PLB2_{APP}$ mice demonstrated slowing of the EEG amidst enhanced theta power when all epochs were pooled rather than stratified by behaviours (see section 3.2). This may indicate dysfunction of the septal-hippocampal pacemaker system. However, regulation of hippocampal theta with speed (and indeed all other parameters) did not differ between $PLB2_{APP}$ and $PLB1_{WT}$ mice. Therefore, while relative Theta amplitude was abnormally enhanced, behavioural modulation of Theta remained intact. It would therefore be of interest for future studies to determine whether pharmacological suppression of abnormally high Theta power in these mice restores locomotive regulation of hippocampal Gamma.

4.2 Gamma power and direction

In our analysis of directional effects on Gamma power, a comparison was made between motion (at the same speed) either towards or away from the Y-maze intersection. Increased Gamma power during inward motion observed here therefore likely relates to cognitive processing associated with approach to a junction rather than an effect of direction *per se.* Increases in CA3 and CA1 local field Gamma power as well as increased coherence between these sites have previously been observed in rats approaching a T-junction (Montgomery and Buzsaki, 2007). Increased fast Gamma power and synchrony between the medial EC and CA1 have also been observed at a maze T-junction specifically prior to execution of a correct arm in a delayed non match to place task (Yamamoto et al., 2014). It is thought that the former finding relates to the retrieval of place cell sequences from the CA3 and transmission to the CA1 in order to plan a future trajectory (Zheng et al., 2016). In the Y-maze spontaneous alternation task, where arm choices are driven by memory of previous arm entries rather than navigation toward a rewarded location, enhanced entrainment of CA1 gamma by the CA3 appears to be the most likely source of elevation in CA1 Gamma during inward motion. Potential dysfunction of the EC may thus be without consequence in the distinction between inward and outward motion but could emerge under analysis of correct vs incorrect alternations. Additionally, if the CA3 is indeed the driver of Gamma power differences between inward and outward motion, this would suggest intact CA3 function in $PLB2_{APP}$ mice which did not differ from $PLB1_{WT}$ in gamma response to direction.

4.3 Spontaneous alternation behaviour

We have previously reported that Theta coherence between the prefrontal cortex and hippocampus is elevated in $PLB1_{WT}$ mice specifically prior to execution of a correct Y-maze alternation (Crouch et al., 2018). We also reported that incorrect alternations were associated with an increase in prefrontal

Gamma power. We hypothesize that the latter finding may represent activity associated with error recognition occurring in the destination arm rather than on approach to the maze intersection. In support of this, we here report that elevated prefrontal Gamma and hippocampal Alpha (relative to correct alternations) are observed during the time where animals have already executed an incorrect arm choice and are moving outward from the maze intersection. It has previously been reported that, in a delayed non-match to place task, synchronization of medial EC and CA1 fast Gamma which would normally occur in the origin arm prior to a correct arm choice occurred in the destination arm, during course correction following an incorrect choice (Yamamoto et al., 2014). These results indicate that the medial EC is involved not only in arm choice but also in error recognition. However, it is not certain to what degree these findings may be applicable to spontaneous vs. rewarded arm choices.

$PLB2_{APP}$ appear to lack the prefrontal (Alpha + Gamma) and Hippocampal (Alpha) EEG responses to incorrect alternations observed in wild type mice despite achieving the same task performance as $PLB1_{WT}$ controls. Unilateral optogenetic silencing of either the left or right CA3 is sufficient to impair spontaneous alternation behaviour (Shipton et al., 2014) indicating a critical role in task performance. However, the majority of information regarding the roles of Individual brain regions in spontaneous alternation behaviour (SAB) is derived mostly from surgical lesioning where damage to the hippocampus, EC, prefrontal cortex and indeed many other regions are all associated with SAB deficits (For review see Lalonde, 2002). Interestingly, rats with electrolytic lesions of the hippocampus can perform above chance in a spontaneous alternation task but fall below chance when the maze is rotated to disrupt the relationship between intra and extra maze cues (Ellen and Deloache, 1968). It is possible therefore that the altered brain activity patterns in the absence of an alternation deficit observed in $PLB2_{APP}$ are due to the adoption of an alternative navigation strategy due to hippocampal dysfunction. However, despite SAB's common use, it must be conceded that the basic scientific concepts underlying rodent behaviour during SAB is overall lacking, and the methods deployed here are unlikely to fully capture and quantify the brain activity associated with arm choices. There is an obvious difficulty in association of oscillatory changes with a particular facet of behaviour where there are no overt changes in behaviour. Identification of the neural systems responsible for SAB should first be based upon (pharmacological) manipulations sufficient to measurably alter behaviour and subsequent investigation of the oscillatory changes which accompany such manipulations. However, such considerations are beyond the purpose of this study. Rather, the EEG profile of $PLB2_{APP}$ during SAB serves as a proof of principle approach to demonstrate that measurement of EEG oscillatory activity during a behavioural task can provide quantifiable indices of brain function and malfunction while overt behavioural readouts are unaffected. This opens a number of possibilities regarding the desire for early phenotype detection in models of dementia, matching calls for improved cognitive testing to overcome the impact of compensation and cognitive reserve in clinical settings.

4.4 Potential translation to Human research

The clearest differentiation between $PLB2_{APP}$ mice and wild type controls emerged through analysis of hippocampal Beta/Gamma response to movement speed. This indicates that rodent hippocampal function can be assessed using measures other than those more typically associated with the hippocampus (memory and cognitive function). Additionally, speed is an entirely objective, quantitative measure and therefore easier to interpret than cognitive readouts (such as spontaneous alternation index) which require some degree of speculation regarding the underlying neuronal/psychological processes. This does raise the question whether similar approaches could be applied to humans.

As the vast majority of the human EEG signal originates from the superficial layers of the neo-cortex, it is not certain to what extent scalp EEG signals, particularly at high frequencies can be attributed to

the human hippocampus. However, using simultaneous magnetoencephalographic (MEG) and intracranial recording, it has been shown that it is possible to resolve high frequency oscillations in the human hippocampus using MEG with appropriate beam forming techniques (Dalal et al., 2013). A recent intracranial recording study found that low frequency oscillations in the human hippocampus are modulated, by both real and virtual movement in a similar manner to that of rodents (Bohbot et al., 2017). A similar approach to our own could therefore be applied in humans using MEG and virtual navigation. However, it was also shown that movement induced theta oscillations occur at lower frequencies during real world vs virtual movement (Bohbot et al., 2017). In rats too, theta frequency increases with speed in a running wheel but not with virtual movement (Ravassard et al., 2013). The speed dependant changes in hippocampal activity reported here may therefore not translate to a virtual environment. Here therefore, EEG carries the advantage of portability which enables studies of real world navigation. However, we are not aware of any studies of relationship of EEG/MEG with (virtual) movement speed in AD patients and are unable to comment on the potential diagnostic value of oscillatory responses to virtual vs real movement. Given the difficulty of recording from the hippocampus with scalp EEG, it is noteworthy that we also observed genotype difference in prefrontal response to correct vs incorrect y-maze alternations. As the prefrontal cortex is more easily accessed using scalp EEG investigation of this feature may be more easily translated to both real and virtual navigation tasks in humans.

4.5 Summary

Synchronization of EEG and behavioural performance combined with intelligent epoch selection can be used to rapidly evaluate brain function associated with a range of behavioural parameters. Even though surface EEG lacks a definite regional precision, it is technically less demanding compared to depth recordings, and modulated by parameters as yet assumed to require LFP recordings. It also appeals from an animal welfare / 3R perspective and offers a translational dimension. Our approach enabled the dissection of state- and behaviour-specific changes alongside the detection of robust regional differences in absolute power.

We here demonstrated the impact of 3 basic parameters on stratified qEEG epochs and their selective impairments in a low-expression AD model. Parameter selection can be easily expanded to more complex behavioural testing and encompass a wide range of task-specific variables. The only salient limit here is the parameters which can be exported from the tracking software. Additionally, analyses of behavioural parameters can be performed post-hoc, without the need for further testing. For example, most tracking software packages allow re-definition of intra-maze zones and boundaries. As infra-red event stamps mark a “real-time” index of each EEG sample, new behaviours such as zone entries and transitions can be retro-actively event-stamped onto an existing EEG record. We therefore propose that such analyses can be incorporated into ‘routine’ home cage or open field superficial EEG recordings to increase both immediate data yield and future reusability.

Declarations of interest:

none

Acknowledgement:

This work was supported by the Alzheimer’s Society [project grant number AS-PG-14-039] to BP and GR.

References

Ahmed, O.J., Mehta, M.R., 2012. Running Speed Alters the Frequency of Hippocampal Gamma Oscillations. J. Neurosci. 32, 7373–7383. https://doi.org/10.1523/JNEUROSCI.5110-11.2012

Ahmed, O.J., Mehta, M.R., 2009. The hippocampal rate code: anatomy, physiology and theory. Trends Neurosci. https://doi.org/10.1016/j.tins.2009.01.009

Bohbot, V.D., Copara, M.S., Gotman, J., Ekstrom, A.D., 2017. Low-frequency theta oscillations in the human hippocampus during real-world and virtual navigation. Nat. Commun. 8. https://doi.org/10.1038/ncomms14415

Braak, H., Braak, E., 1991. Neuropathological stageing of Alzheimer-related changes. Acta Neuropathol. 82, 239–259. https://doi.org/10.1007/BF00308809

Bush, D., Bisby, J.A., Bird, C.M., Gollwitzer, S., Rodionov, R., Diehl, B., McEvoy, A.W., Walker, M.C., Burgess, N., 2017. Human hippocampal theta power indicates movement onset and distance travelled. Proc. Natl. Acad. Sci. 114, 12297–12302. https://doi.org/10.1073/pnas.1708716114

Buzsáki, G., 2002. Theta oscillations in the hippocampus. Neuron. https://doi.org/10.1016/S0896-6273(02)00586-X

Chen, Z., Resnik, E., McFarland, J.M., Sakmann, B., Mehta, M.R., 2011. Speed controls the amplitude and timing of the Hippocampal Gamma rhythm. PLoS One 6. https://doi.org/10.1371/journal.pone.0021408

Coben, L.A., Danziger, W., Storandt, M., 1985. A longitudinal EEG study of mild senile dementia of Alzheimer type: changes at 1 year and at 2.5 years. Electroencephalogr. Clin. Neurophysiol. 61, 101–112. https://doi.org/10.1016/0013-4694(85)91048-X

Colgin, L.L., 2016. Rhythms of the hippocampal network. Nat. Rev. Neurosci. https://doi.org/10.1038/nrn.2016.21

Colgin, L.L., Denninger, T., Fyhn, M., Hafting, T., Bonnevie, T., Jensen, O., Moser, M.B., Moser, E.I., 2009. Frequency of gamma oscillations routes flow of information in the hippocampus. Nature 462, 353–357. https://doi.org/10.1038/nature08573

Crispin-Bailey, C., Moulds, A., Platt, B., Hollier, G.P., Freeman, M.J., Fargus, A.G., 2013. A Miniaturized 4-Channel, 2KSa/sec Biosignal Data Recorder With 3-Axis Accelerometer and Infra-red Timestamp Function.

Crouch, B., Sommerlade, L., Veselcic, P., Riedel, G., Schelter, B., Platt, B., 2018. Detection of time-, frequency- and direction-resolved communication within brain networks. Sci. Rep. 8, 1825. https://doi.org/10.1038/s41598-018-19707-1

Dalal, S., Jerbi, K., Bertrand, O., Adam, C., Ducorps, A., Schwartz, D., Martinerie, J., Lachaux, J.-P., 2013. Simultaneous MEG-intracranial EEG: New insights into the ability of MEG to capture oscillatory modulations in the neocortex and the hippocampus. Epilepsy Behav. 28, 283–302. https://doi.org/10.1016/j.yebeh.2013.03.012

Drinkenburg, W.H.I.M., Ruigt, G.S.F., Ahnaou, A., 2016. Pharmaco-EEG Studies in Animals: An Overview of Contemporary Translational Applications. Neuropsychobiology. https://doi.org/10.1159/000442210

Ellen, P., Deloache, J., 1968. Hippocampal lesions and spontaneous alternation behavior in the rat. Physiol. Behav. 3, 857–860. https://doi.org/10.1016/0031-9384(68)90167-4

Etholm, L., Arabadzisz, D., Lipp, H.P., Heggelund, P., 2010. Seizure logging: A new approach to

synchronized cable-free EEG and video recordings of seizure activity in mice. J. Neurosci. Methods 192, 254–260. https://doi.org/10.1016/j.jneumeth.2010.08.003

Faust, O., Acharya, R.U., Allen, A.R., Lin, C.M., 2008. Analysis of EEG signals during epileptic and alcoholic states using AR modeling techniques. ITBM-RBM 29, 44–52. https://doi.org/10.1016/j.rbmret.2007.11.003

Freund, T.F., Antal, M., 1988. GABA-containing neurons in the septum control inhibitory interneurons in the hippocampus. Nature 336, 170–173. https://doi.org/10.1038/336170a0

Fu, H., Rodriguez, G.A., Herman, M., Emrani, S., Nahmani, E., Barrett, G., Figueroa, H.Y., Goldberg, E., Hussaini, S.A., Duff, K.E., 2017. Tau Pathology Induces Excitatory Neuron Loss, Grid Cell Dysfunction, and Spatial Memory Deficits Reminiscent of Early Alzheimer's Disease. Neuron 93, 533–541.e5. https://doi.org/10.1016/j.neuron.2016.12.023

Hamm, V., Héraud, C., Cassel, J.-C., Mathis, C., Goutagny, R., 2015. Precocious Alterations of Brain Oscillatory Activity in Alzheimer's Disease: A Window of Opportunity for Early Diagnosis and Treatment. Front. Cell. Neurosci. 9. https://doi.org/10.3389/fncel.2015.00491

Hinman, J.R., Dannenberg, H., Alexander, A., Hasselmo, M.E., 2018. Neural mechanisms of navigation involving interactions of cortical and subcortical structures. J. Neurophysiol. https://doi.org/10.1152/jn.00498.2017

Hughes, R.N., 2004. The value of spontaneous alternation behavior (SAB) as a test of retention in pharmacological investigations of memory. Neurosci. Biobehav. Rev. https://doi.org/10.1016/j.neubiorev.2004.06.006

Jeong, J., 2004. EEG dynamics in patients with Alzheimer's disease. Clin. Neurophysiol. https://doi.org/10.1016/j.clinph.2004.01.001

Khan, U.A., Liu, L., Provenzano, F.A., Berman, D.E., Profaci, C.P., Sloan, R., Mayeux, R., Duff, K.E., Small, S.A., 2014. Molecular drivers and cortical spread of lateral entorhinal cortex dysfunction in preclinical Alzheimer's disease. Nat. Neurosci. 17, 304–311. https://doi.org/10.1038/nn.3606

Klein, A.S., Donoso, J.R., Kempter, R., Schmitz, D., Beed, P., 2016. Early Cortical Changes in Gamma Oscillations in Alzheimer's Disease. Front. Syst. Neurosci. 10. https://doi.org/10.3389/fnsys.2016.00083

Kropff, E., Carmichael, J.E., Moser, M.B., Moser, E.I., 2015. Speed cells in the medial entorhinal cortex. Nature 523, 419–424. https://doi.org/10.1038/nature14622

Lalonde, R., 2002. The neurobiological basis of spontaneous alternation. Neurosci. Biobehav. Rev. https://doi.org/10.1016/S0149-7634(01)00041-0

Leiser, S.C., Dunlop, J., Bowlby, M.R., Devilbiss, D.M., 2011. Aligning strategies for using EEG as a surrogate biomarker: A review of preclinical and clinical research. Biochem. Pharmacol. https://doi.org/10.1016/j.bcp.2010.10.002

McFarland, W.L., Teitelbaum, H., Hedges, E.K., 1975. Relationship between hippocampal theta activity and running speed in the rat. J. Comp. Physiol. Psychol. 88, 324–328. https://doi.org/10.1037/h0076177

Montgomery, S.M., Buzsaki, G., 2007. Gamma oscillations dynamically couple hippocampal CA3 and CA1 regions during memory task performance. Proc. Natl. Acad. Sci. 104, 14495–14500. https://doi.org/10.1073/pnas.0701826104

Moretti, D. V., Fracassi, C., Pievani, M., Geroldi, C., Binetti, G., Zanetti, O., Sosta, K., Rossini, P.M., Frisoni, G.B., 2009. Increase of theta/gamma ratio is associated with memory impairment. Clin.

Neurophysiol. 120, 295–303. https://doi.org/10.1016/j.clinph.2008.11.012

Moser, E.I., Kropff, E., Moser, M.-B., 2008. Place Cells, Grid Cells, and the Brain's Spatial Representation System. Annu. Rev. Neurosci. 31, 69–89. https://doi.org/10.1146/annurev.neuro.31.061307.090723

Nakazono, T., Lam, T.N., Patel, A.Y., Kitazawa, M., Saito, T., Saido, T.C., Igarashi, K.M., 2017. Impaired In Vivo Gamma Oscillations in the Medial Entorhinal Cortex of Knock-in Alzheimer Model. Front. Syst. Neurosci. 11. https://doi.org/10.3389/fnsys.2017.00048

Paxinos, G., Franklin, K.B.J., 2004. The mouse brain in stereotaxic coordinates, Academic Press. https://doi.org/10.1016/S0306-4530(03)00088-X

Platt, B., Drever, B., Koss, D., Stoppelkamp, S., Jyoti, A., Plano, A., Utan, A., Merrick, G., Ryan, D., Melis, V., Wan, H., Mingarelli, M., Porcu, E., Scrocchi, L., Welch, A., Riedel, G., 2011a. Abnormal cognition, sleep, eeg and brain metabolism in a novel knock-in alzheimer mouse, plb1. PLoS One 6. https://doi.org/10.1371/journal.pone.0027068

Platt, B., Welch, A., Riedel, G., 2011b. FDG–PET imaging, EEG and sleep phenotypes as translational biomarkers for research in Alzheimer's disease. Biochem. Soc. Trans. 39, 874–880. https://doi.org/10.1042/BST0390874

Plucińska , K., Crouch, B., Koss, D., Robinson, L., Siebrecht, M., Riedel, G., Platt, B., 2014. Knock-In of Human BACE1 Cleaves Murine APP and Reiterates Alzheimer-like Phenotypes. J. Neurosci. 34, 10710–10728. https://doi.org/10.1523/JNEUROSCI.0433-14.2014

Plucińska, K., Crouch, B., Yeap, J., Stoppelkamp, S., Riedel, G., Platt, B., *In press*. Histological and behavioural phenotypes of a novel mutated APP knock-in mouse.

Ravassard, P., Kees, A., Willers, B., Ho, D., Aharoni, D., Cushman, J., Aghajan, Z.M., Mehta, M.R., 2013. Multisensory control of hippocampal spatiotemporal selectivity. Science (80-.). 340, 1342–1346. https://doi.org/10.1126/science.1232655

Schomburg, E.W., Fernández-Ruiz, A., Mizuseki, K., Berényi, A., Anastassiou, C.A., Koch, C., Buzsáki, G., 2014. Theta Phase Segregation of Input-Specific Gamma Patterns in Entorhinal-Hippocampal Networks. Neuron 84, 470–485. https://doi.org/10.1016/j.neuron.2014.08.051

Shipton, O.A., El-Gaby, M., Apergis-Schoute, J., Deisseroth, K., Bannerman, D.M., Paulsen, O., Kohl, M.M., 2014. Left–right dissociation of hippocampal memory processes in mice. Proc. Natl. Acad. Sci. 111, 15238–15243. https://doi.org/10.1073/pnas.1405648111

Thompson, B.L., Levitt, P., Stanwood, G.D., 2005. Prenatal cocaine exposure specifically alters spontaneous alternation behavior. Behav. Brain Res. 164, 107–116. https://doi.org/10.1016/j.bbr.2005.06.010

Watrous, A.J., Fried, I., Ekstrom, A.D., 2011. Behavioral correlates of human hippocampal delta and theta oscillations during navigation. J. Neurophysiol. 105, 1747–1755. https://doi.org/10.1152/jn.00921.2010

Yamamoto, J., Suh, J., Takeuchi, D., Tonegawa, S., 2014. Successful execution of working memory linked to synchronized high-frequency gamma oscillations. Cell 157, 845–857. https://doi.org/10.1016/j.cell.2014.04.009

Zheng, C., Bieri, K.W., Hsiao, Y.T., Colgin, L.L., 2016. Spatial Sequence Coding Differs during Slow and Fast Gamma Rhythms in the Hippocampus. Neuron 89, 398–408. https://doi.org/10.1016/j.neuron.2015.12.005

Figure legends

Figure 1: Plots of inward vs outward motion samples.

Plots display examples of motion paths (black lines) during EEG epochs where animals achieved >= 50cm displacement towards (Inward) or away from (Outward) the centre point of the Y-maze. Blue and red markers at either end of each motion path represent the animal's location at the start and end of the epoch respectively. Each maze arm is 60cm in length.

Figure 2: Y-maze cognitive and locomotor measures.

A) Spontaneous alternation scores in $PLB1_{WT}$ (black) vs $PLB2_{APP}$ (red) mice. Numbers of occurrences of correct alternations (CA), incorrect alternations (IA), and direct repetitions (DR) are expressed as % total alternations (Mean + SEM). Text on plot summarizes p values for effects of genotype (Geno), Alternation type (Alt), and interaction (Int). **B)** Total distance moved [m] by each animal over the course of the 10 minute y-maze trial. **C)** Average speed of each animal [cm/s] calculated from distance data presented in B. Text above horizontal bars in B and C indicate results of comparison between genotypes (ns = $p>0.05$).

Figure 3: General spectral power differences between $PLB1_{WT}$ and $PLB2_{APP}$ mice in Y-maze environment.

A) Mean + SEM absolute EEG power [Log AR a.u] recorded from the prefrontal cortex of $PLB1_{WT}$ (black) vs $PLB2_{APP}$ (red) over 10 minutes in the Y-maze (averaged over 4 second epochs). Text on plot provides p value summary for overall effects of Genotype (Geno), Frequency (Freq) and interaction (Int). **B)** Data in A normalized to total power **C)** Absolute EEG power [Log AR a.u] recorded from the hippocampus. **D)** Data in C normalized to total power. Asterisks on C and D represent p-values for effect of genotype over associated frequency bands *** = $p<0.001$.

Figure 4: Relationship between movement speed and EEG power in $PLB1_{WT}$ and $PLB2_{APP}$ mice.

A) Relative power spectrum displaying magnitude (Mean + SEM) of difference in prefrontal EEG power between speed bin 1 (S1) and speed bin 5 (S5) for $PLB1_{WT}$ (black) vs $PLB2_{APP}$ (red) mic**e.** Values above 1 indicate higher power at speed S5, values below 1 indicate higher power at speed S1. **B)** Effect of speed on prefrontal relative band power. Text on plot summarizes p-values for effect of genotype (Geno), Power band (Band), and interaction (Int). Asterisks above data points indicate significant effects of genotype in Bonferronni post-tests. **C**) Correlation between movement speed and prefrontal Gamma band power. Asterisks next to genotype labels indicate a significant speed-power correlation. **D,E,F)** Same information as A,B,C provided for the hippocampal recording site. * = $p<0.05$, ** = $p<0.01$.

Figure 5: Relationship between movement speed and hippocampal peak Theta & Beta power in $PLB1_{WT}$ and $PLB2_{APP}$ mice.

A) Correlation between movement speed and peak Theta power in the hippocampus. **B)** Correlation between movement speed and peak hippocampal beta power. Asterisks beside genotype labels summarize p-values of tests for correlation between power and speed. * = p<0.05, ** = p<0.01.

Figure 6: EEG power during motion towards vs motion away from Y-maze centre

A) Effect of direction on prefrontal EEG band power. Values above 1 indicate band power is greater during inward movements, values below 1 indicate greater power during outward movements. Text on plot summarizes p-values for effect of genotype (Geno), Power band (Band), and interaction (Int). **B)** Scatter plots elaborating effect of direction specifically on prefrontal Gamma band power. Asterisks above genotype labels summarize p values of one-sample t-tests against a chance level of 1 (no effect of direction). Text above horizontal bars indicates result of t-test between genotypes. **C & D)** Same analyses as A and B respectively conducted for hippocampal recording site. * = p<0.05, ** p<0.01.

Figure 7: EEG power during correct vs incorrect alternations in the Y-maze

A) Effect of alternation type on prefrontal EEG band power. Values above 1 indicate band power is greater during incorrect alternations, values below 1 indicate greater power during correct alternations. Text on plot summarizes p-values for effect of genotype (Geno), Power band (Band), and interaction (Int). Asterisks above data points indicate significant effects of genotype in Bonferronni post-tests. **B,C)** Scatter plots elaborating effect of direction specifically on prefrontal Alpha (B) and Gamma (C) band power. Asterisks above genotype labels summarize p values of one-sample t-tests against a chance level of 1 (no effect of alternation type). Text above horizontal bars indicates result of t-test between genotypes. **D,E,F)** Same analyses as A, B and C respectively conducted for hippocampal recording site. * = p<0.05, ** p<0.01.

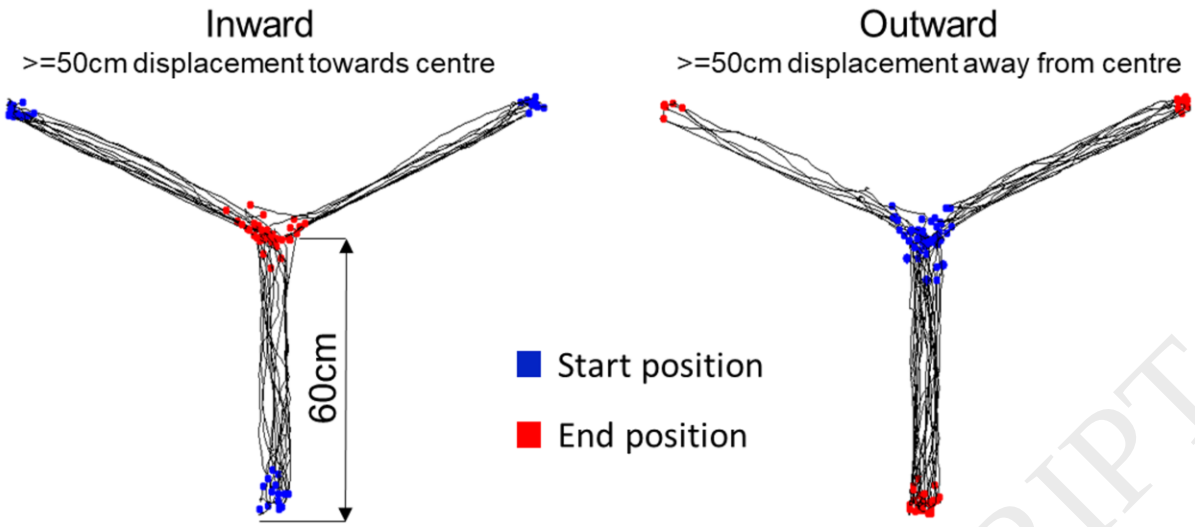

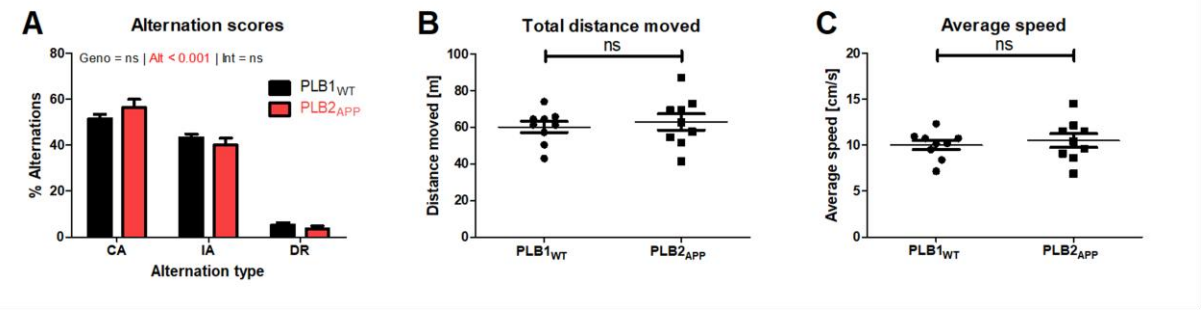

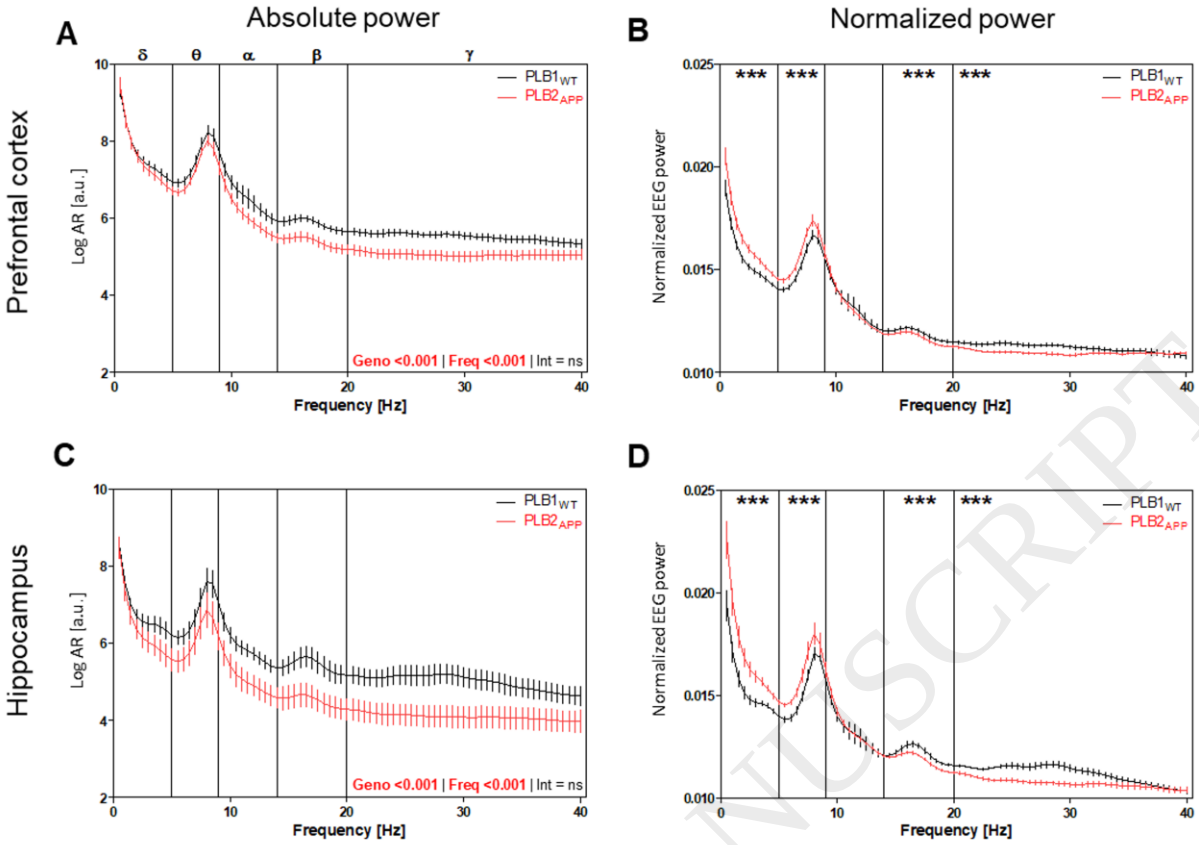

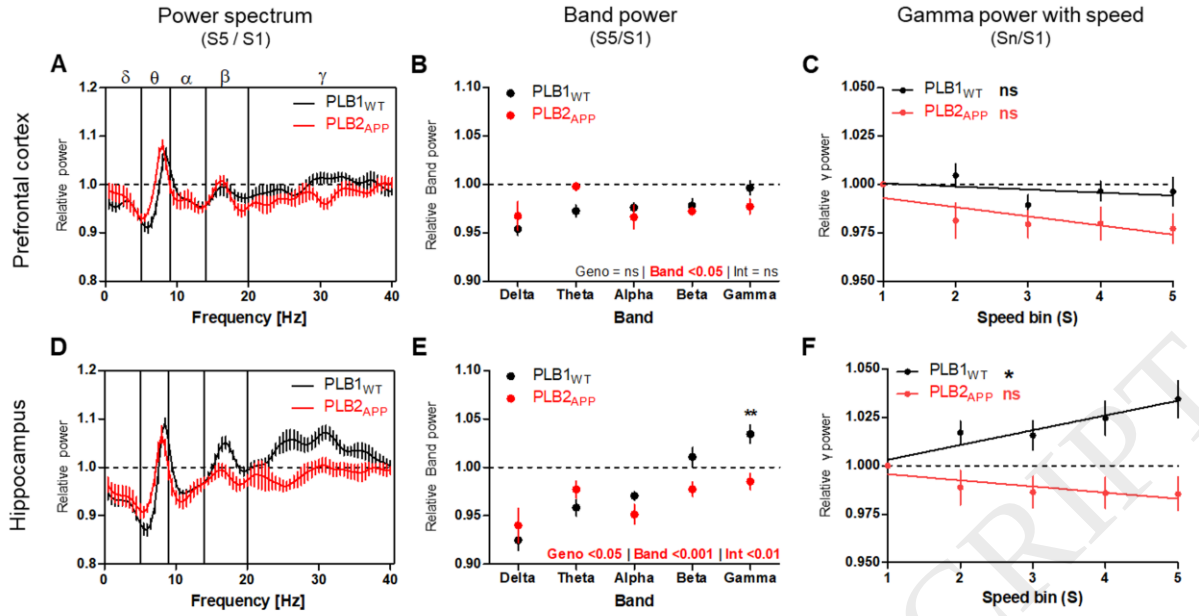

Speed bin	S1	S2	S3	S4	S5
Speed range [cm/s]	0 – 3.2	3.2 – 6.4	6.4 – 9.6	9.6 – 12.8	12.8 – 16

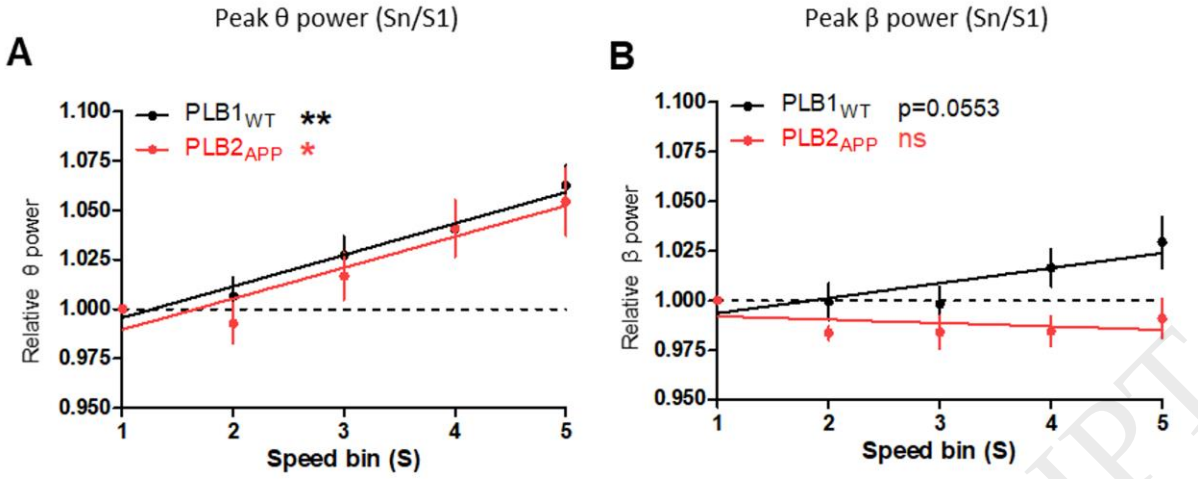

Speed bin	S1	S2	S3	S4	S5
Speed range [cm/s]	0 – 3.2	3.2 – 6.4	6.4 – 9.6	9.6 – 12.8	12.8 – 16